Biochemical and Biophysical Research Communications 382 (2009) 205–209

Contents lists available at ScienceDirect

Biochemical and Biophysical Research Communications

journal homepage: www.elsevier.com/locate/ybbrc

Functional aberration of myofibrils by cardiomyopathy-causing mutations in the coiled-coil region of the troponin-core domain

Fumiko Matsumoto [a], Kayo Maeda [b], Toshiyuki Chatake [c], Yuichiro Maéda [b,d,*], Satoru Fujiwara [a,*]

[a] Quantum Beam Science Directorate, Japan Atomic Energy Agency, 2-4 Shirakata-Shirane, Tokai-mura, Naka-gun, Ibaraki 319-1195, Japan
[b] ERATO Project 'Actin Filament Dynamics', Japan Science and Technology Agency, Sayo, Hyogo 679-5148, Japan
[c] Kyoto University Research Reactor Institute, Kumatori-cho, Sennan-gun, Osaka 590-0494, Japan
[d] Structural Biology Research Center and Division of Biological Science, Graduate School of Science, Nagoya University, Furo-cho, Nagoya 464-8602, Japan

ARTICLE INFO

Article history:
Received 19 February 2009
Available online 9 March 2009

Keywords:
Troponin
Cardiomyopathy
Muscle regulation
ATPase activity
Hydrogen bond
Molecular dynamics

ABSTRACT

Two cardiomyopathy-causing mutations, E244D and K247R, in human cardiac troponin T (TnT) are located in the coiled-coil region of the Tn-core domain. To elucidate effects of mutations in this region on the regulatory function of Tn, we measured Ca^{2+}-dependent ATPase activity of myofibrils containing various mutants of TnT at these residues. The results confirmed that the mutant E244D increases the maximum ATPase activity without changing the Ca^{2+}-sensitivity. The mutant K247R was shown for the first time to have the effect similar to the mutant E244D. Furthermore, various TnT mutants (E244D, E244M, E244A, E244K, K247R, K247E, and K247A) showed various effects on the maximum ATPase activity while the Ca^{2+}-sensitivity was unchanged. Molecular dynamics simulations of the Tn-core containing these TnT mutants suggested that the hydrogen-bond network formed by the side chains of neighboring residues around residues 244 and 247 is important for Tn to function properly.

In vertebrate striated muscles, muscle contraction is regulated in a Ca^{2+}-sensitive manner by troponin (Tn) and tropomyosin (Tm), located on the actin-containing thin filaments [1]. Tn is a complex consisting of three subunits; TnC, TnI, and TnT. Binding of Ca^{2+} to TnC triggers a series of conformational changes of TnC, TnI, TnT, and Tm that release inhibition of interaction between myosin and actin, thereby allowing muscle contraction to occur. Mutations at various locations in Tn may have effects on various points along the pathway of the conformational changes, thereby having various effects on the regulatory function. Indeed, more than 60 mutations of Tn have been shown to cause various types of cardiomyopathy [2,3]. Understanding how the mutations of Tn affect the regulatory function is therefore important to understand not only the mechanism of pathogenesis of cardiomyopathy but also the regulatory mechanism by Tn.

Effects of the disease-causing mutants of Tn on Ca^{2+}-regulation have been investigated using the techniques by which intrinsic Tn within isolated skinned fibers and myofibrils is replaced with recombinant Tn [4,5]. The effect of the mutant Tn has been shown to be classified into three types; increasing the Ca^{2+}-sensitivity without altering the maximal force (type I) [6–8], decreasing the Ca^{2+}-sensitivity without altering the maximal force (type II) [9,10], and increasing the maximal force without altering the Ca^{2+}-sensitivity (type III) [11,12]. Most of the mutations showing the effects of the type I and II are located in the regions directly involved with Ca^{2+}-regulation such as Tm-binding region, the actin-binding region, and the regulatory region of TnC [2,3]. However, two mutations of TnT, E244D, and K247R, one of which (E244D) was found to have the effect of the type III [2], are located in the region not directly involved with Ca^{2+}-regulation. They are located in the coiled-coil region formed by TnI and TnT (the IT arm) of the Tn-core domain [13]. Since this IT arm connects the region containing Ca^{2+}-binding site of TnC and Tm-binding region of TnT, this region may play a pivotal role related to propagation of the Ca^{2+}-binding signal from TnC to Tm. Elucidating how the mutations in this region affect the regulatory function should thus provide insights into not only the regulatory mechanism by Tn but also the mechanism of the functional aberration of the type III.

Here, to investigate the effects of the mutations at residues 244 and 247 of TnT on the regulatory function, we prepared various recombinant TnTs mutated at these residues, incorporated them into myofibrils, and measured Ca^{2+}-dependent ATPase activity. We also calculated structural models of the Tn-core containing the mutant TnTs by molecular dynamics (MD) simulations to gain insights into the effects of the mutations on the local structure of Tn. A relationship between the functional aberration caused by the mutations

* Corresponding authors. Fax: +81 52 747 6433 (Y. Maéda); fax: +81 29 282 5822 (S. Fujiwara).
E-mail addresses: ymaeda@nucc.cc.nagoya-u.ac.jp (Y. Maéda), fujiwara.satoru@jaea.go.jp (S. Fujiwara).

0006-291X/$ - see front matter © 2009 Elsevier Inc. All rights reserved.
doi:10.1016/j.bbrc.2009.03.009

and the local structures around the mutated residues was suggested.

Materials and methods

Cloning and mutagenesis of human cardiac Tn cDNAs. Human cardiac (hc) cDNA bank was purchased from GIBCOBRL. Cloning of hcTnI was carried out by PCR using following oligos; the forward primer was 5′-CTCACCATGGCCGATGGTAGCAGCGATGCGG-3′ with the NcoI site and the reverse primer was 5′-GGCAGGATCCCTC AGCTCTCAAACTTTTTCTTGCGGCCC-3′ with BamHI site. PCR fragment was digested by NcoI and BamHI and cloned into pTV118 which was also digested both by NcoI and BamHI. Cys97 and Cys80 were changed to Ala using Mutan-K (Takara). After the mutagenesis, pTV118 TnI(C80A,C97A) was digested by NcoI and BamHI and cloned into pET3d which was cleaved also both by NcoI and BamHI. Cloning of TnT was carried out by PCR using following oligos: the forward primer was 5′-GGTGGTGGAAGCGTACGAAG AGG-3′ with SplI site and the reverse primer was 5′-GCTGCAGGA TCCTATTTCCAGCGCCCGG-3′ with BamHI site. PCR fragment was digested by SplI and BamHI and ligated with pET3d which was digested both by NcoI and BamHI and following oligos 5′-CATGTC TGACATCGAAG-3′ and 5′-GTACTCTTCCACCTCTTCTTCGATGTCAG A-3′, giving rise to pETTnT. Cloning and mutagenesis of cys leit hcTnC cDNA were carried out as described [13]. Mutagenesis of TnT(E244D), TnT(E244A), TnT(E244K), TnT(E244M), TnT(K247R), TnT(K247A), TnT(K247E), were carried out using QuikChange II Site-Directed Mutagenesis Kit (Stratagene), using pETTnT as a template.

Expression and purification of recombinant Tns. The recombinant hcTnTs were expressed in *Escherichia coli* BL21-CodonPlus(DE3)-RP. The harvested cells by centrifugation were resuspended in solution containing 50 mM Tris–HCl (pH 7.5), 5 mM EDTA, 20% sucrose and 0.5 mg/ml lysozyme and incubated for 1 h at 4 °C. After repeated sonication on ice, the supernatant was brought to contain 6 M urea, 0.1 M NaCl, and 5 mM 2-mercaptoethanol. The hcTnTs were purified by SP Sepharose FF (GE Healthcare) and DEAE Sepharose FF (GE Healthcare), followed by RESOURCE RPC (GE Healthcare) using a linear gradient from 1% to 90% of acetonitrile. The wild-type cysteineless variants of hcTnI and hcTnC were expressed in *E. coli* BL21(DE3)-pLys-S. The hcTnI was purified by SP Sepharose FF, followed by RESOURCE RPC. Purification of the hcTnC was performed as described [14].

Preparation of myofibrils containing mutant Tns. Myofibrils were prepared from bovine heart according to the method of Solaro et al. [15], and stored at −20 °C in solution containing 50% glycerol, 20 mM MOPS (pH 7.0), 60 mM KCl and 2 mM $MgCl_2$. Stocked myofibrils were resuspended in a solution containing 60 mM KCl and 1 mM $NaHCO_3$ just before use. The recombinant TnT was first exchanged into myofibrils, and the recombinant TnI and TnC were then reconstituted into myofibrils [11].

ATPase activity measurements. The ATPase activity measurements, the reaction times of which were 30 min, were done at various pCa(−log[Ca^{2+}]) values between 4.5 and 7.0 as described [11]. The pCa values were calculated by using the stability constant of $8.45 \times 10^5\ M^{-1}$ for Ca^{2+}–EGTA [16]. To determine the pCa value at half-maximal ATPase activity (pCa_{50}) and the Hill coefficient (n_H), the relative ATPase activity was analyzed by fitting with the Hill equation (relative ATPase activity (%) = 100/{1 + 10^(pCa − pCa_{50})n_H}) as described [6]. The maximum ATPase activity of myofibrils containing each mutant was normalized to the maximum ATPase activity of myofibrils containing the wild-type hcTnT in the same series of the measurements.

Electrophoresis. SDS–PAGE was carried out according to the procedure of Laemmli [17] at an acrylamide concentration of 12.5%. The gels were stained with 0.1% Coomassie brilliant blue G250. Densitometric analysis was performed using the public domain NIH Image (version 1.62) program (developed at the U.S. National Institutes of Health and available at http://rsb.info.nih.gov/nih-image/).

Molecular dynamics simulations. Two coordinates of the Tn-core structure are available (PDB Accession Code: 1J1D and 1J1E) [13]. We employed the 1J1D structure because this structure was obtained from the crystallographic data with better resolution (2.6 Å, compared to the resolution of 3.3 Å for 1J1E). The 1J1D structure contains two molecules of the Tn-core. We term the structure consisting of the chains A, B, and C in 1J1D as 1J1Da, and that consisting of the chains D, E, and F as 1J1Db. Both structures were employed as the starting structures separately. Residues 1–91 of TnC and residues 183–225 and 272–288 of TnT(183–288) were removed from the coordinates because these residues are rather separated from the dense region including the IT arm, thereby having little effects on the structure of the IT arm region. These truncated structures of 1J1Da and 1J1Db were used as the starting structures. MD simulations were performed using the program NAMD (version 2.6) [18] with the CHARM22 force-field parameters and visualizing program VMD [19]. The starting structure was placed in a water sphere with a radius of 46 Å with a periodic boundary condition. Energy minimization was done for 2000 steps. The mutation was generated in this energy-minimized structure by the model-building software Coot [20]. Energy minimization of the mutated structure was done for 2000 steps. MD (50 ps) was then performed with an integration time step of 2 fs under the conditions of constant pressure (1 atm) and temperature (310 K). The equilibrium of the system was attained at about 5.6 ps. The coordinates after the equilibrium were stored every 0.1 ps and the average coordinates were calculated from these stored structures.

Results and discussion

Displacement of TnT mutants in myofibrils

Fig. 1 shows the SDS–PAGE patterns of the purified wild-type hcTnT, cardiomyopathy-causing hcTnT mutants (TnT(E244D) and

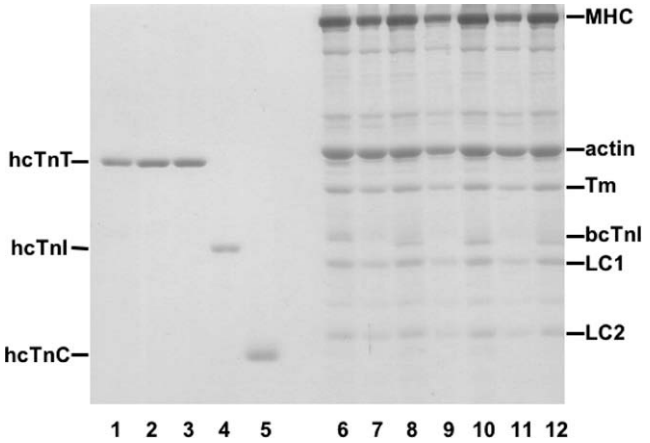

Fig. 1. SDS–PAGE patterns of bovine cardiac myofibrils before and after exchange with recombinant hcTnT, TnI and TnC. Lane1, purified wild-type hcTnT; lane 2, purified hcTnT(E244D); lane 3, purified hcTnT(K247R); lane 4, purified hcTnI; lane 5, purified hcTnC; lane 6, untreated myofibrils; lane 7, myofibrils treated with wild-type hcTnT; lane 8, myofibrils treated with wild-type hcTnT and reconstituted with hcTnI and hcTnC; lane 9, myofibrils treated with hcTnT(E244D); lane 10, myofibrils treated with hcTnT(E244D) and reconstituted with hcTnI and hcTnC; lane 11, myofibrils treated with TnT(K247R); and lane 12, myofibrils treated with hcTnT(K247R) and reconstituted with hcTnI and hcTnC. MHC, LC1, LC2, and bcTnI denote myosin heavy chain, myosin light chain 1, myosin light chain 2, and intrinsic bovine cardiac TnI, respectively.

TnT(K247R)), hcTnI and hcTnC (lanes 1–5). Each Tn component shows a single band, indicating that there are no appreciable impurities or degradations. Gels of other hcTnT mutants prepared also gave single bands, indicating that the preparations of these mutants have similar quality to the wild-type and cardiomyopathy-causing TnTs (data not shown). These recombinant hcTnTs and hcTnC show similar electrophoretic mobility to bcTnT and bcTnC while the recombinant hcTnI shows somewhat faster mobility than the native bcTnI.

Fig. 1 also shows the patterns during the reconstitution of myofibrils containing the recombinant hcTn components. The bands from the endogenous Tn-complex disappeared from the pattern by the TnT treatment (lanes 7, 9, 11), and the bands from the recombinant TnI and TnC appeared after the reconstitution (lanes 8, 10, 12). Densitometric analysis of these patterns showed that the exchange rate of the endogenous Tn with the recombinant TnT was approximately 65%, consistent with the previous reports [11]. The exchange rates were similar in all the recombinant TnTs, and the amounts of the incorporated hcTnI and hcTnC were similar to the amounts of the endogenous TnI and TnC.

Effects of the cardiomyopathy-causing mutants on the ATPase activity

The ATPase activity measurements of myofibrils containing the wild-type hcTnT and those containing the cardiomyopathy-causing mutants of hcTnT (E244D and K247R) were performed at various pCa values. Fig. 2A and B shows the pCa-dependence of the ATPase activity, from which the maximum ATPase activity relative to myofibrils containing the wild-type TnT, the pCa value at half-maximal activity (pCa_{50}), and the Hill coefficient (n_H) were estimated. The parameter values obtained are summarized in Table 1. The maximum ATPase activity of myofibrils containing TnT(E244D) was 109.4 ± 4.5% of that of myofibrils containing the wild-type TnT, but there were no significant differences in pCa_{50} and n_H. This indicates that this mutant has the effect of the type III, confirming the previous studies [11,12].

The effect of the other mutant TnT(K247R) that causes cardiomyopathy [21] has not yet been analyzed. Here, as shown in Fig. 2B and Table 1, the maximum ATPase activity of myofibrils containing this mutant was 112.9 ± 6.6% of that of myofibrils containing the wild-type TnT, while no appreciable differences in pCa_{50} and n_H were observed. The mutant TnT(K247R) is thus shown for the first time to have the effect of the type III.

The mutants that has been shown to have the effect of the type III so far are TnT(E244D) [11,12], TnT(K247R) (this study), and TnT(F110I) [22]. Residue 110 is located in the domain TnT1, which binds to Tm [23,24], suggesting that the effect of the type III is related to the Tn–Tm interactions. Thus, the mutations at residues 244 and 247 of TnT should also affect the Tn–Tm interactions though the IT arm region, in which residues 244 and 247 are located, has no direct contacts with Tm. It has been suggested that the region around residues 244 and 247 is critical in the structure and dynamics of the Tn-core: the coiled-coil structure is bent in this region, and the side chains of the charged residues at 244 and 247, which should usually be hydrophobic and form a hydrophobic core between the helices, protrude from the hydrophobic core to form a hydrogen-bond network with neighboring residues, suggesting that the coiled-coil structure is destabilized in this region [25]. It is therefore important to investigate how the mutations at these residues affect the regulatory function. We thus introduced various mutations at residues 244 and 247, and measured the ATPase activity of myofibrils containing these mutants.

Effects of various hcTnT mutants on the ATPase activity

We introduced various mutations that could affect the hydrogen-bond network in various ways. In addition to the cardiomyopathy-causing mutants, TnT(E244D) and TnT(K247R), the mutants TnT(E244M), TnT(E244A), TnT(E244K), TnT(K247E), and TnT(K247A), were prepared. TnT(E244D) has the same negative charge but a smaller volume: TnT(E244M) is hydrophobic and has a larger volume; TnT(E244A) is hydrophobic but has a smaller

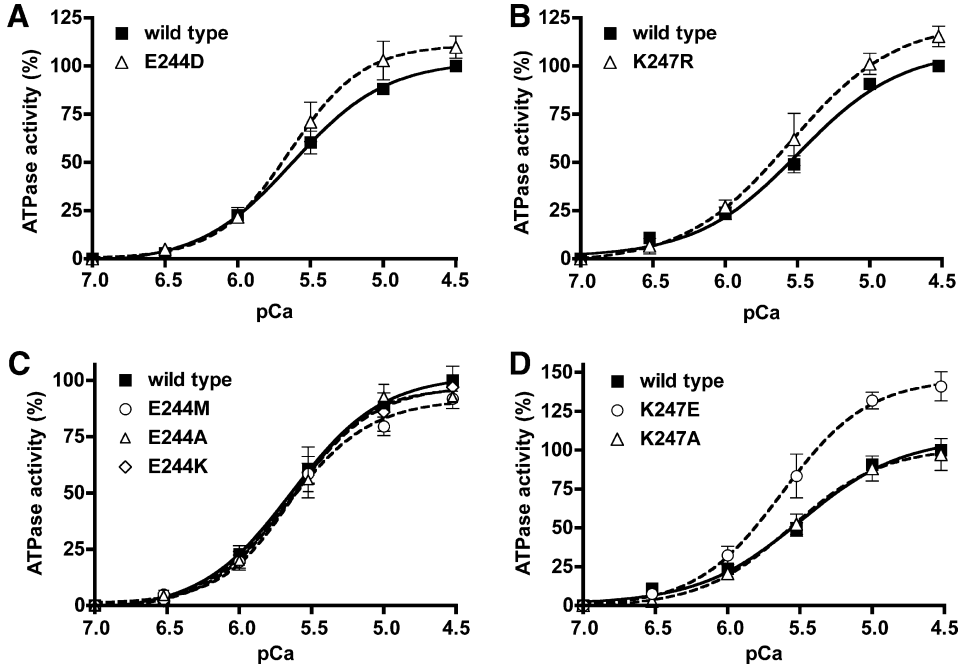

Fig. 2. Dependence on pCa^{2+} of the relative ATPase activity of myofibrils containing various hcTnT mutants, normalized to the averaged maximum ATPase activity of myofibrils containing the wild-type TnT. The activities of myofibrils containing A; the mutant E244D(TnT) (open triangles), B; the mutant K247R(TnT) (open triangles), C; the mutants E244M(TnT) (open circles), E244A(TnT) (open triangles), and E244K(TnT) (open diamonds), and D; the mutants K247E(TnT) (open circles) and K247A(TnT) (open triangles), are shown. At each panel, the results of myofibrils containing the wild-type TnT (filled squares) are shown as a standard. Solid and dashed lines denote the fits with the Hill equation. Means and standard deviations of three (TnT (E244X) mutants) or four (TnT(K247X) mutants) independent series of the measurements are shown.

Table 1
Ca^{2+}-sensitivity, maximum ATPase activity, and cooperativity in recombinant hcTnT-exchanged myofibrils.

TnT	pCa_{50}	Maximum ATPase activity (%)	n_H
Wild type	5.62 ± 0.03	100.0 ± 0.0	1.50 ± 0.13
E244D	5.63 ± 0.04	109.4 ± 4.5	1.75 ± 0.26
E244A	5.64 ± 0.03	95.9 ± 2.9	1.75 ± 0.21
E244K	5.62 ± 0.03	96.7 ± 6.5	1.57 ± 0.29
E244M	5.64 ± 0.03	90.2 ± 3.0[a]	1.48 ± 0.29
Wild type	5.58 ± 0.03	100.0 ± 0.0	1.40 ± 0.13
K247R	5.59 ± 0.05	112.9 ± 6.6[b]	1.38 ± 0.22
K247A	5.60 ± 0.06	96.5 ± 6.1	1.54 ± 0.25
K247E	5.65 ± 0.05	140.0 ± 7.3[a]	1.58 ± 0.28

Values are means ± S.E. of three (E244X series) or four (K247X series) independent series of measurements. [a]$P < 0.01$, and [b]$P < 0.05$ vs. wild-type (t-test).

volume; TnT(E244K) has the opposite (positive) charge and a larger volume; TnT(K247R) has the same positive charge but a larger volume; TnT(K247E) has the opposite (negative) charge and a smaller volume; and TnT(K247A) is hydrophobic and has a smaller volume.

Fig. 2C and D shows the pCa-dependence of the ATPase activity of myofibrils containing these mutants. The parameters obtained are shown in Table 1. While no appreciable effects were observed in pCa_{50} for all the mutants measured, indicating that these mutants have no Ca^{2+}-sensitizing effects, various effects were observed on the maximum ATPase activity. TnT(E244A), TnT(E244K), TnT(E244M), and TnT(K247A) appears to have a tendency to have lower maximum ATPase activity than the wild type. Although this tendency may be small in TnT(E244A), TnT(E244K), and TnT(K247A), TnT(E244M) showed rather clear tendency of the decreased maximum activity. On the other hand, TnT(K247E) showed significantly larger maximum ATPase activity. It was larger than that of the cardiomyopathy-causing mutant TnT(K247R).

The results obtained here showed no apparent tendencies to depend on the volumes, charges, or hydrophobicity of the mutated residues. Thus, to understand the effects of these mutations, the structure of the Tn-core, particularly the local structure including the hydrogen-bond network around the mutated residues, should be inspected. Since the crystal structures of the Tn-core containing the mutant TnTs are not available yet, we performed molecular dynamics (MD) simulations to calculate the structural models of the Tn-cores containing the mutant TnTs.

Effects of the mutations on the local structure of the IT arm

Fig. 3 shows the averaged local structures around residues 244 and 247 of TnT, calculated from the MD simulations. Fig. 3A shows the structure of the wild type. It is shown that an extensive hydrogen-bond network are formed between residues K106(TnI), E110(TnI), K247(TnT), E244(TnT), R79(TnI), and R103(TnI). However, in TnT(E244D), TnT(K247R), and TnT(K247E), which show the effect of increasing the maximum ATPase activity, this hydrogen-bond network appears to be perturbed: the hydrogen bond between E110(TnI) and residue 247 of TnT is broken, and the hydrogen bond formed by R103(TnI) is altered (Fig. 3C, F, and G). These perturbations are clearly observed in the structures

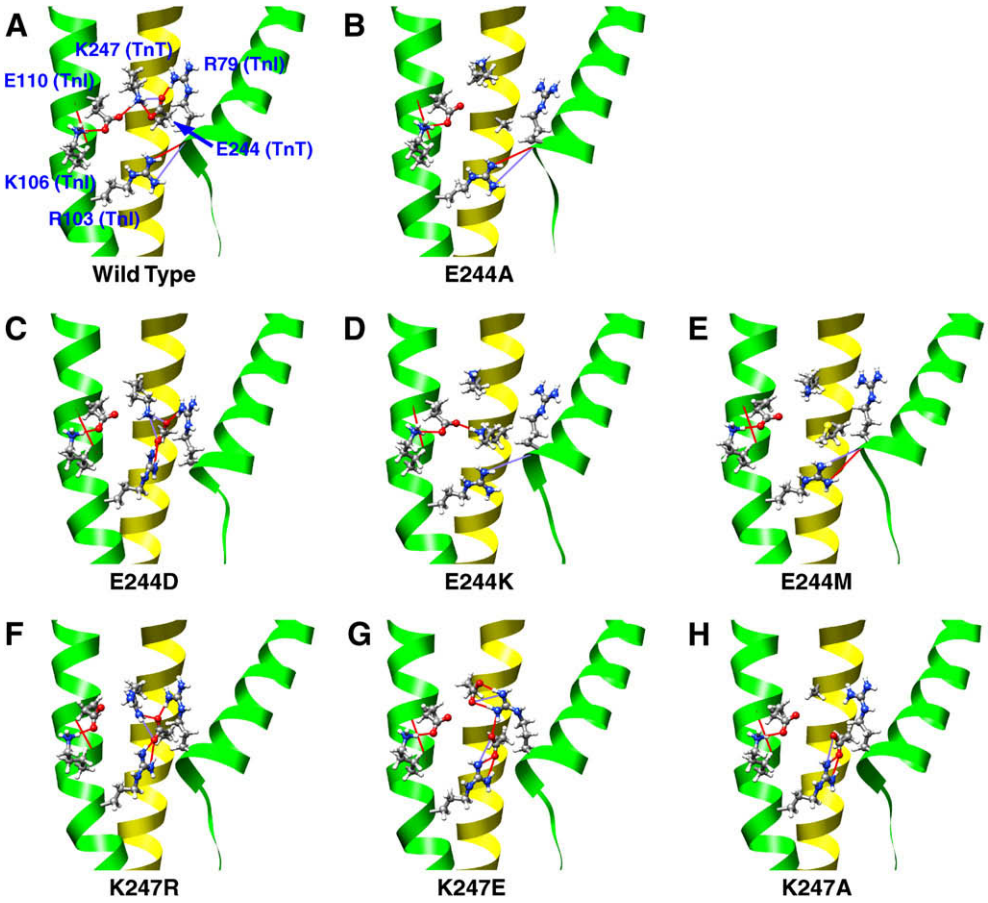

Fig. 3. Models of the local structures around residues 244 and 247 of TnT of the Tn-core containing various mutant TnTs. Averaged structures calculated from the trajectories of 50-ps MD simulations are shown. Ribbon diagrams in yellow and green represent the backbone structures of TnT and TnI, respectively. Solid lines in red denote the hydrogen bonds that meet the criteria [26] and those in violet denote the hydrogen bonds, criteria of which are relaxed by 0.4 Å and 20°. The images were produced using the program package for the molecular modeling, UCSF Chimera [27].

calculated from the starting structure 1J1Db. The effects observed in the structures from 1J1Da were subtler: in TnT(E244D) and TnT(K247R), the hydrogen bond between R103(TnI) and R79(TnI) was not broken but weakened, i.e., the distance between the hydrogen donor and acceptor was larger than that in the wild type (results not shown). Tendency of weakening the hydrogen bonds are, however, the same in the structures from 1J1Da and 1J1Db. The overall effect of these mutants thus appears to be weakening the hydrogen network.

In the structures of TnT(E244A), TnT(E244K), TnT(E244M), and TnT(K247A), which have the effect of rather decreasing the maximum ATPase activity, the hydrogen-bond network is disrupted rather completely (Fig. 3B, D, E, and H). These effects are similar in both the structures calculated from 1J1Da and 1J1Db.

These observations imply that the "proper" function of Tn requires fine tuning of the hydrogen-bond network formed by residues 244 and 247 of TnT and neighboring residues. Small perturbations of this hydrogen-bond network result in the increase of the maximum ATPase activity, and the disruption of the hydrogen-bond network has the opposite effect of decreasing the activity. This demonstrates the importance of this hydrogen-bond network in the function of Tn related particularly to the signal propagation from TnC to Tm. The small perturbation of this local hydrogen-bond network may be amplified to induce large conformational changes so that the pathway of the signal propagation from TnC to Tm is influenced. Elucidation of how such conformational changes could be induced by the mutations requires the structure analysis of Tn containing the mutant TnT, which is currently underway.

Acknowledgments

We thank Drs. S. Morimoto, F. Takahashi-Yanaga, and Y. Nitanai for technical advices and discussions. We also thank Prof. I. Ohtsuki for valuable discussions and encouragement.

References

[1] S. Ebashi, M. Endo, I. Ohtsuki, Control of muscle contraction, Q. Rev. Biophys. 2 (1969) 351–384.
[2] K. Harada, S. Morimoto, Inherited cardiomyopathies as a troponin disease, Jpn. J. Physiol. 54 (2004) 307–318.
[3] M.X. Li, X. Wang, B.D. Sykes, Structural based insights into the role of troponin in cardiac muscle physiology, J. Muscle Res. Cell Motil. 25 (2004) 559–579.
[4] F. Shiraishi, M. Kambara, I. Ohtsuki, Replacement of troponin components in myofibrils, J. Biochem. 111 (1992) 61–65.
[5] M. Hatakenaka, I. Ohtsuki, Replacement of three troponin components with cardiac troponin components within single glycerinated skeletal muscle fibers, Biochem. Biophys. Res. Commun. 181 (1991) 1022–1027.
[6] S. Morimoto, H. Nakaura, F. Yanaga, I. Ohtsuki, Functional consequences of a carboxyl terminal missense mutation Arg278Cys in human cardiac troponin T, Biochem. Biophys. Res. Commun. 261 (1999) 79–82.
[7] K. Harada, F. Takahashi-Yanaga, R. Minakami, S. Morimoto, I. Ohtsuki, Functional consequences of the deletion mutation ΔGlu160 in human cardiac troponin T, J. Biochem. (Tokyo) 127 (2000) 263–268.
[8] S. Morimoto, F. Yanaga, R. Minakami, I. Ohtsuki, Ca^{2+}-sensitizing effects of the mutations at Ile-79 and Arg-92 of troponin T in hypertrophic cardiomyopathy, Am. J. Physiol. 275 (1998) C200–C207.
[9] S. Morimoto, Q.W. Lu, K. Harada, F. Takahashi-Yanaga, R. Minakami, M. Ohta, T. Sasaguri, I. Ohtsuki, Ca^{2+}-desensitizing effect of a deletion mutation Delta K210 in cardiac troponin T that causes familial dilated cardiomyopathy, Proc. Natl. Acad. Sci. USA 99 (2002) 913–918.
[10] P. Robinson, M. Mirza, A. Knott, H. Abdulrazzak, R. Willott, S. Marston, H. Watkins, C. Redwood, Alterations in thin filament regulation induced by a human cardiac troponin T mutant that causes dilated cardiomyopathy are distinct from those induced by troponin T mutants that cause hypertrophic cardiomyopathy, J. Biol. Chem. 277 (2002) 40710–40716.
[11] F. Yanaga, S. Morimoto, I. Ohtsuki, Ca^{2+} sensitization and potentiation of the maximum level of myofibrillar ATPase activity caused by mutations of troponin T found in familial hypertrophic cardiomyopathy, J. Biol. Chem. 274 (1999) 8806–8812.
[12] K. Harada, J.D. Potter, Familial hypertrophic cardiomyopathy mutations from different functional regions of troponin T result in different effects on the pH and Ca^{2+} sensitivity of cardiac muscle contraction, J. Biol. Chem. 279 (2004) 14488–14495.
[13] S. Takeda, A. Yamashita, K. Maeda, Y. Maéda, Structure of the core domain of human cardiac troponin in the Ca^{2+}-saturated form, Nature 424 (2003) 35–41.
[14] F. Matsumoto, K. Makino, K. Maeda, H. Patzelt, Y. Maéda, S. Fujiwara, Conformational changes of troponin C within the thin filaments detected by neutron scattering, J. Mol. Biol. 342 (2004) 1209–1221.
[15] R.J. Solaro, D.C. Pang, F.N. Briggs, The purification of cardiac myofibrils with Triton X-100, Biochim. Biophys. Acta 245 (1971) 259–262.
[16] H. Harafuji, Y. Ogawa, Re-examination of the apparent binding constant of ethylene glycol bis(beta-aminoethyl ether)-*N*,*N*,*N*′,*N*′-tetraacetic acid with calcium around neutral pH, J. Biochem. 87 (1980) 1305–1312.
[17] U.K. Laemmli, Cleavage of structural proteins during the assembly of the head of bacteriophage T4, Nature 227 (1970) 680–685.
[18] J.C. Phillips, R. Braun, W. Wang, J. Gumbart, E. Tajkhorshid, E. Villa, C. Chipot, R.D. Skeel, L. Kale, K. Schulten, Scalable molecular dynamics with NAMD, J. Comput. Chem. 26 (2005) 1781–1802.
[19] W. Humphrey, A. Dalke, K. Schulten, VMD—visual molecular dynamics, J. Mol. Graph. 24 (1996) 33–38.
[20] P. Emsley, K. Cowtan, Coot: model-building tools for molecular graphics, Acta Crystallogr. D 60 (2004) 2126–2132.
[21] O.M. Hernandez, P.R. Housmans, J.D. Potter, Pathophysiology of cardiac muscle contraction and relaxation as a result of alterations in thin filament regulation, J. Appl. Physiol. 90 (2001) 1125–1136.
[22] H. Nakaura, F. Yanaga, I. Ohtsuki, S. Morimoto, Effects of missense mutations Phe110Ile and Glu244Asp in human cardiac troponin T on force generation in skinned cardiac muscle fibers, J. Biochem. 126 (1999) 457–460.
[23] J.R. Pearlstone, L.B. Smillie, Binding of troponin-T fragments to several types of tropomyosin. Sensitivity to Ca^{2+} in the presence of troponin-C, J. Biol. Chem. 257 (1982) 10587–10592.
[24] M. Tanokura, Y. Tawada, A. Ono, I. Ohtsuki, Chymotryptic subfragments of troponin T from rabbit skeletal muscle. Interaction with tropomyosin, troponin I and troponin C, J. Biochem. 93 (1983) 331–337.
[25] Y. Maéda, Y. Nitanai, T. Oda, From the crystal structure of troponin to the mechanism of calcium regulation of muscle contraction, Adv. Exp. Med. Biol. 592 (2007) 37–46.
[26] J.E.J. Mills, P.M. Dean, Three-dimensional hydrogen-bond geometry and probability information from a crystal survey, J. Comput. Aided Mol. Des. 10 (1996) 607–622.
[27] E.F. Pettersen, T.D. Goddard, C.C. Huang, G.S. Couch, D.M. Greenblatt, E.C. Meng, T.E. Ferrin, UCSF Chimera—a visualization system for exploratory research and analysis, J. Comput. Chem. 25 (2004) 1605–1612.